https://doi.org/10.5194/cp-2024-79
Preprint. Discussion started: 16 December 2024

Climate of the Past Discussions

Alternating cold and warm periods during the European late-Holocene

Evelien J.C. van Dijk[1,2], Christoph C. Raible[1], Michael Sigl[1], Johann Jungclaus[3], and Heinz Wanner[1]

[1]Department of Physics and the Oeschger Center for Climate Change Research, University of Bern, Switzerland
[2]Department of Geosciences, University of Oslo, Norway
[3]Max Planck Institute for Meteorology, Hamburg, Germany

Correspondence: Evelien J.C. van Dijk (e.van.dijk@geo.uio.no)

Abstract. The decadal to centennial scale climate variability of the past 4000 years consists of colder and warmer periods, potentially initiated by fast varying external forcing, or the lack thereof. These alternating cold and warm periods are most clearly visualized by the waxing and waning of glaciers in the Northern Hemisphere. However, these cold and warm periods are neither spatially nor temporally consistent, and using these defined periods to interpret local variations in climate and society could prove difficult. Here, we use two global earth system models, as well as available proxy reconstructions to examine to which extent the defined warm and cold periods of the last 4000 years before the industrial period are reflected in the climate for Northern, Southern, and Central Europe. We find that on regional scales, the relative role of internal variability appears more pronounced compared to the externally forced signal, thereby decreasing the forcing signal in local climate records. In addition, one model suggests that the climate variability for Northern Europe follows the external forcing more closely than the climate of Central and especially Southern Europe, while the other model shows rather ambiguous results. This study illustrates that periods defined by glacier advances and archaeology have to be carefully used in the interpretation of past events at a local scale, as it is likely that internal variability dominates on such scales.

1 Introduction

The present inter-glacial, called Holocene, covers approximately the last 11,700 years. The early, the mid, and the late-Holocene, with the latter usually defined at the 4.2 ka event (Walker et al., 2012). Under the term "Holocene temperature conundrum" the question is asked whether the global temperature trend after the Holocene Thermal Maximum between about 8000 and 5000 years before present (BP) (Renssen et al., 2012) was negative or positive (Wanner, 2021).

Climate modelling studies typically show a positive trend of global temperatures over the Holocene and do not depict a mid-Holocene temperature maximum (Liu et al., 2014; Tian et al., 2022; Hopcroft et al., 2023; van Dijk et al., 2024). Bader et al. (2020) showed that warming mainly affects the tropics. A long term cooling trend predominates in the high-latitudes summer, which is primarily due to orbital forcing. This negative temperature trend in the Northern Hemisphere extra-tropics during the last 4000 years was superimposed by multi-decadal to century-long fluctuations between warmer and colder phases (Mayewski et al., 2004; Essell et al., 2023; van Dijk et al., 2024). Studies based on proxy networks show decreasing global temperatures following a vaguely defined Holocene Thermal Maximum (Cartapanis et al., 2022), though there is an ongoing debate to which

https://doi.org/10.5194/cp-2024-79
Preprint. Discussion started: 16 December 2024


Climate of the Past Discussions

extent long-term trends are influenced by existing biases in spatial and seasonal representation of the underlying proxies (Kaufman et al., 2004; Charpentier Ljungqvist, 2011; Marcott et al., 2013; Baker et al., 2017; Marsicek et al., 2018; Kaufman et al., 2020; Bova et al., 2021; Kaufman and Broadman, 2023). The reference to a cooler Late Holocene, which is linked to the term Neoglacial, originally comes from Porter and Denton (1967), who reconstructed multi-century glacier advances and retreats in the North American Cordillera. Increasing glacier growth is evident over the last 5000 years (Oerlemans, 2005; Holzhauser et al., 2005; Solomina et al., 2015; Palacios et al., 2023). The archaeological and historical literature took note of them early on and studied the effects of these climatic swings on early human societies (Weiss and Bradley, 2001; Haldon, 2016; Bernard et al., 2023). The warm and cold phases studied for the European climate for the Late Holocene are shown in Table 1 with reference to selected key publications. Note that we provide previously defined climatic events by their given name using the ka BP notation (relative to 1950 CE) but otherwise report the dates using the BCE/CE notation. All radiocarbon dates are calibrated against the calibration curve recommended at the time of publication.

The 4.2 ka event, which marks the transition to the Late Holocene, is characterised by the strong decline of the summer monsoons, especially in the Afro-Asian region. The associated extreme dry periods led in part to the collapse of advanced civilizations in the Sahara (Manning and Timpson, 2014), Egypt (Weldeab et al., 2014), Mesopotamia, India and China (Staubwasser and Weiss, 2006). Bradley and Bakke (2019) and McKay et al. (2024) confirmed that there was no compelling evidence for a significant and widespread climate anomaly around 2200 BCE in the European area. This is also confirmed by Roland et al. (2014) for the British Isles and Ireland. Jalali and Sicre (2019) pointed out that a mega drought occurred in the eastern Mediterranean basin.

The series of late Holocene cold and warm periods in Europe was initiated around 1700 BCE by a cooling, the so-called "Loebben Oscillation" (Patzelt and Bortenschlager, 1973), which manifested itself in the central Tyrolean Alps (Stubai valley) in a two-phase moraine system around 1700 ($\pm$ 330) BCE and 1190 ($\pm$ 280) BCE (Moran et al., 2017). Jørgensen and Riede (2019) described the so-called and concurrent termination of the Gressbakken Phase in Arctic Norway, which coincided with a population decline at the end of the Stone Age. The temperature decline peaked around 1600 BCE, and was associated with an increase in precipitation and a strong forest decline. Volcanic activity and climate forcing were strongly elevated between 1660 and 1560 BCE with this period including some of the largest caldera-forming eruptions such as Aniakchak and Thera (Sigl et al., 2022; Pearson et al., 2022).

The Bronze Age Warm Period following the Loebben Oscillation was less pronounced but is reflected in several climate reconstructions. The temperature reconstruction from the southern boreal zone of Finland by Heikkilä and Seppä (2003), based on pollen stratigraphy, results in significantly elevated temperatures for the time shortly before 1050 BCE. Holzhauser et al. (2005) showed that the largest glacier in the Alps, the Aletsch Glacier, had melted back relatively far before 950 BCE. Le Roy et al. (2015) also referred to the phase between 1450 and 1200 BCE as the Bronze Age Warm Period based on the glacier

https://doi.org/10.5194/cp-2024-79
Preprint. Discussion started: 16 December 2024


Climate of the Past Discussions

retreat at the Mer de Glace in the Mont Blanc massif.

The subsequent cooling was relatively strong. It exists in the literature under the title "2.8 ka event". Martin-Puertas et al. (2012) pointed out that a Grand Solar Minimum, often called Homeric Minimum, and the associated reduction in ultraviolet radiation likely played an important role. They concluded that the cooling is massive mainly because the atmospheric circulation amplified the solar signal. In addition large volcanic eruptions may compounded the cooling occurring e.g. in 723, 648, 572 and 426 BCE. This cold phase is also documented by glacier advances. Zoller (1966) analysed it in the Göschenertal valley of the central Swiss Alps and referred to it as Göschenen I. Their study is questioned by Boxleitner et al. (2019), but there is clear evidence of glacier advances at the Aletsch Glacier (Holzhauser et al., 2005, Fig 2) and at the Mer de Glace (Le Roy et al., 2015).

The cold 2.8 ka event was followed by the Iron – Roman Age Warm Period. McCormick et al. (2012) described the period between 100 BCE and 200 CE in particular as warm and stable with hardly any extreme events. They attributed this calm climate phase to a low level of volcanic activity and stable solar irradiance. In the context of the past 2,500 years volcanic activity between 40 BCE and 200 CE was exceptionally quiescent and has been referred to as the "Roman Quiet Period" (Manning et al., 2017; Sigl et al., 2022). Temperature reconstructions from Europe based on tree-rings show general warm conditions and a lower frequency of cold years (Büntgen et al., 2011; Luterbacher et al., 2016). Margaritelli et al. (2020) clearly demonstrated in their reconstruction of sea surface temperatures in the Sicily Channel that temperatures between 1 CE and 500 CE were up to 2°C higher than the long-term mean. Not surprisingly the analyses of the glaciers by Holzhauser et al. (2005) in the central and western Alps generally show significant melting during the Iron - Roman Age warm period.

The subsequent massive cooling period has been given several names. In the classical literature it is called the Dark Ages Cold Period (DACP). Helama et al. (2017) have analysed 114 paleoclimate papers and describe the period from 400 to 765 CE as typical for the DACP. It was not only cold, but also wet, with the exception of the Mediterranean region. Büntgen et al. (2016) named the period from 536 to 660 CE the Late Antique Little Ice Age (LALIA). Based on their dendrochronological analysis, they described the summer temperatures during the LALIA as unprecedented, long-lasting, spatially synchronized and more severe than all summer cold phases of the Little Ice Age. Consistent with other authors (Sigl et al., 2015; Toohey et al., 2016; Van Dijk et al., 2022) they attributed large volcanic eruptions especially in 536 and 540 CE and subsequent large eruptions in the 6th and 7th century as the trigger for this cold phase and postulated a duration of up to 660 CE promoting glacier advances in the Northern Hemisphere. Very occasionally, the cold phase is called the Vandal Minimum. It is also very prominently represented in the glaciological literature and is often referred to as Göschenen II. Le Roy et al. (2015) demonstrated two advances at Mer de Glace in the Mont Blanc massif around 337 CE and 606 CE. Boxleitner et al. (2019) named the period 1.8 to 1.1 ka for Göschenen II, and Holzhauser et al. (2005) identified a larger advance around 600 CE after a very small advance of the Aletsch glacier around 300 CE (Fig. 2).

https://doi.org/10.5194/cp-2024-79
Preprint. Discussion started: 16 December 2024


Climate of the Past Discussions

Lamb (1965) first mentioned the following warmer period from about 1000 to 1200 CE, which he called the "medieval warm epoch", mainly on the basis of documentary data. Later the terms Medieval Climate Anomaly (MCA) or Medieval Warm Period (MWP) were used. Hughes and Diaz (1994) showed that, depending on the method of analysis, temporally different periods appear to be warmer, and Bradley et al. (2003) demonstrated that warming of several tenths of a degree also occurred in a regionally differentiated manner. Based on numerous new studies, Diaz et al. (2011) proposed the period 950 to 1400 CE for the duration of the MWP. Bradley et al. (2016) suggested that, during a 'Medieval Quiet Period' (725-1025 CE), the climate system was relatively unperturbed by natural forcing factors (i.e. the absence of large tropical volcanic eruptions, solar irradiance minima), resulting in a unique period of climate stability. However, it was recently shown by Gabriel et al. (2024) that volcanic activity in Iceland surged during an 'Icelandic Active Period' (750-940 CE), promoting frequent climate extremes and famines across medieval Europe (McCormick et al., 2007; Haldon et al., 2018)

The term "Little Ice Age" (LIA) was first used by (Matthes, 1939). He used it to refer to the resurgence of glaciers in the Sierra Nevada region of California in connection with the onset of cooling after the Holocene Thermal Maximum (Renssen et al., 2012; Marcott et al., 2013). On the century timescale, it is possible that the LIA was the coldest period of the last 8000 years. In her monograph on the LIA, Grove (1988) referred primarily to the European glacial advances and placed the beginning in the 13th century. Wanner et al. (2022) proposed a period from 1350 to 1860 CE for Europe. Using proxy data and available instrument measurements, they estimated seasonal temperatures and showed that the LIA was primarily based on very low winter temperatures. Matthews and Briffa (2005) pointed out the fact, also discussed in glaciological studies, that individual periods had higher humidity. After the middle of the 19th century, there is the gradual transition from the Little Ice Age to the Modern Warm Period.

The so-defined cold and warm periods originate from the field of archaeology, or from glacial advances in the Alps and/or Scandinavia. However, climate is a complex system and cold and warm periods such as those that occurred during the late Holocene rarely cover the entire globe or an entire hemisphere. For the LIA, studies suggested that the spatial extent and duration, as well as the timing, was heterogeneous across the NH (Mann, 2002; Wanner et al., 2022; Matthews and Briffa, 2005). We therefore expect, that these defined warm and cold periods have more nuance to them, and will not necessarily be homogeneous events across the NH, or even an entire continent. For this study, we focus on Europe, as there is proficient coverage of paleoproxy reconstructions and glacier advances. In addition, we will use transient model simulations with the Max Planck Institute Earth system model (MPI-ESM) and the Community Earth system model (CESM).

2 Data and Methods

2.1 Glacier curves

The glacier curves used in this study are from Jostedalsbreen (Nesje et al., 2001; Nesje, 2009; Vasskog et al., 2012) in Norway, and the Aletsch glacier and Mer de Glace (Holzhauser et al., 2005; Le Roy et al., 2015) in the Alps. These glaciers are some of the largest glaciers in Europe and have been studied extensively.

https://doi.org/10.5194/cp-2024-79
Preprint. Discussion started: 16 December 2024

Climate of the Past Discussions

Period ID	Period name	Temporal allocation	Climatic character	Key literature
4.2 ka event	4.2 ka event	∼2200 BCE	No remarkable anomaly	Roland et al. (2014) Bradley and Bakke (2019) Jalali and Sicre (2019)
3.6 ka event	Loebben Oscillation / Gressbakken Phase	1700-1200 BCE	Small to medium-sized glacier advances in the Alps	Patzelt and Bortenschlager (1973) Moran et al. (2005) Jorgensen and Riede (2019)
BWP	Bronze Age Warm Period	Shortly before 1000 BCE	Warm and partly dry	Heikkila and Seppa (2003) Holzhauser et al. (2005) Le Roy et al. (2015)
2.8 ka event	2.8 ka event / Homeric Minimum / Göschenen I	∼1000-300 BCE	Cool and humid	Martin-Puertas et al. (2012) Boxleitner et al. (2019)
RWP	Iron-Roman Age Warm Period	250 BCE - 400 CE	Stable warm and dry	McCormick et al. (2012) Margaritelli et al. (2020)
DACP	Dark Age Cooling LALIA Göschenen II Vandal Minimum	400 - 750 CE	Cold and partly humid	Lamb (1965) Hughes and Diaz (1994) Bradley et al. (2016) Diaz et al. (2011)
MWP	Medieval Warm Period	∼950 - 1400 CE	Warm period	Diaz et al. (2011)
LIA	Little Ice Age	1250-1860 CE	Cold	Matthews and Briffa (2005) Wanner et al. (2022)

Table 1. The warm and cold phases studied for the European climate for the Late Holocene.

The glacier curves are determined from individual data distributed irregularly over time. For the Great Aletsch Glacier written and pictorial historical records such as drawings, paintings, engravings and photographs have been interpreted. In addition, the radiocarbon dating of fossil soils and wood from glacier fore-fields also indicate glacier advance and retreat periods. The dendrochronological analysis of trees raised by the advancing glacier allowed the authors to determine absolute dates if they fit within known absolute dated tree-ring chronologies (Holzhauser et al., 2005). For the reconstruction of the Mer de Glace curve, tree-rings of wood fragments from precisely identified moraines were very carefully analysed and their age determined (radiocarbon dated, especially using smaller wood fragments) (Le Roy et al., 2015). For Jostedalsbreen, the Equilibrium Line Altitude (ELA) were determined by magnetic susceptibility in sediment cores from a proglacial lake. The magnetic susceptibility was correlated with the sediment transport, the glacier size and, thus, the net balance of the ice mass (Nesje et al., 2000).

The Aletsch Glacier in the Valais Alps in Switzerland is the largest Alpine glacier with a length of 20 km and an area of 80 km^2 (Jouvet and Huss, 2019). The Mer de Glace in the Chamonix valley has a length of 11.5 km and an area of 30.4 km^2

https://doi.org/10.5194/cp-2024-79
Preprint. Discussion started: 16 December 2024

Climate of the Past Discussions

(Le Roy et al., 2015). The Jostedalsbreen had an area of 458 km^2 in 2019 (Nesje, 2009)(Nesje and Matthews, in prep.). The location of the glaciers can be found in Fig.1.

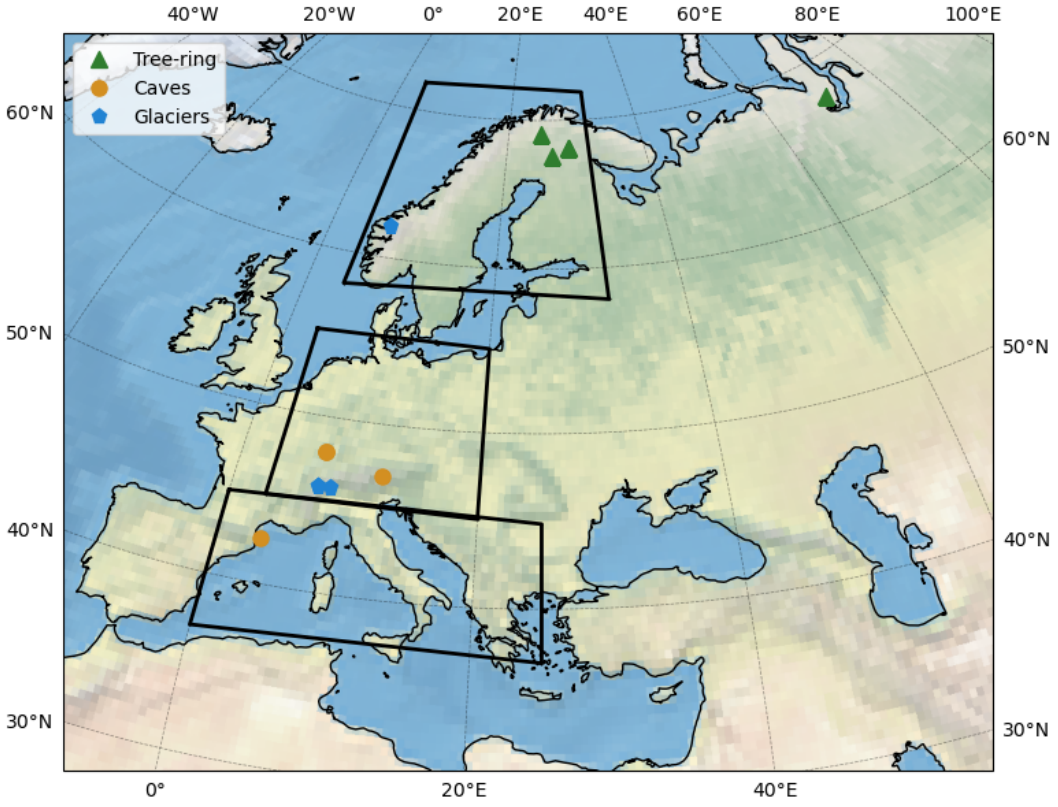

Figure 1. Map with the location of the tree-ring proxies (green triangles), the speleothems (orange dots), and the glaciers (blue hexagons), as well as the spatial domain for Northern Europe, Central Europe, and Southern Europe as used in this study.

2.2 Proxy reconstructions

We also use available proxy reconstructions with high temporal resolution (annual to decadal scale; Table 2). Anomalies are calculated for each proxy reconstruction by subtracting the mean of the 1500 BCE to 1850 CE period from the time series, after which the 100-year mean is calculated. We take the 100-year mean to allow a comparison with the glacier curves.

For the temperature limited areas in the high-latitudes, we use tree-ring records to study the temperature variations in the late-Holocene. For Central- and Southern Europe, speleothem records are used. Most of the available data sets are given as anomalies with respect to 1-1850 CE, except for the speleothem records from Austria, which are given as $\delta^{18}O$. A list with information about the records can be found in Table 2, and the locations can be found in Fig. 1.

https://doi.org/10.5194/cp-2024-79
Preprint. Discussion started: 16 December 2024

Climate of the Past Discussions

Site	Archive	Proxy	Location	lat/lon	Season	Source
		TRW / pollen	Lapland	69°N, 25°E	Summer	Helama et al. (2010)
		TRW	Torneträsk	68°N, 20°E	Summer	Grudd et al. (2002)
		TRW	Siberia	67-68°N, 70-71°E	Summer	Hantemirov et al. (2023)
		TRW	Finland	67-70°N, 24-29°E	Summer	Helama et al. (2022)
Milandre	Fluid inclusions	$\delta^{18}O$	Switzerland	48°N, 7°E	Annual	Affolter et al. (2019)
Spannagle	Calcite	$\delta^{18}O$	Austria	47°N, 12°E	Annual	Fohlmeister et al. (2012)
	Calcite	Speleothems$\delta^{18}O$	Spain	42-43°N, 3-4°E	Annual	Martin-Chivelet et al. (2011)
		TRW	Northern Hemispere	30-90°N, -180-180°E	Summer	Büntgen et al. (2021)

Table 2. Information for the different proxy data sets used for Fig. 3. TRW corresponds to Tree Ring Width.

2.3 Model simulations

The cold and warm periods defined by archaeological and proxy evidence are compared to model simulations. We use simulations from two fully coupled earth system models spanning 1500 BCE to 1850 CE.

The first model is the Max Planck Institute Earth Sytem Model (MPI-ESM) version 1.2 (Mauritsen et al., 2019). This model features a T63 horizontal resolution ($1.9° \times 1.9°$) for the atmospheric component (ECHAM6) and a vertical resolution of 47 levels between the surface and top of the atmosphere at 80 km (0.01 hPa) (Stevens et al., 2013). The ocean component (MPIOM) has a nominal horizontal resolution of $1.5°$ and 40 vertical levels (Jungclaus et al., 2013). Two transient simulations were carried out for the Holocene, spanning the mid to late-Holocene (6000 BCE to 1850 CE). The difference between the two simulations is in the forcing. One simulation includes prescribed variations in orbital forcing (Berger, 1978) and greenhouse gas concentrations (Brovkin et al., 2019; Köhler, 2019) (the `orbital + GHG` simulation), and the other simulation includes land use changes (Hurtt et al., 2020), stratospheric ozone (varies with solar irradiance, (Bader et al., 2020)), solar irradiance (Krivova et al., 2011) and stratospheric volcanic aerosol (Sigl et al., 2022) in addition (the `all forcing` simulation). The spin-up simulation was simulation with constant conditions at 6000 BCE. More information on the model setup and the Holocene simulation can be found in (Dallmeyer et al., 2021).

The second model is the Community Earth System Model (CESM) version 1.2.2 (Hurrell et al., 2013). The model consists of the atmospheric component CAM5 (Community Atmosphere Model version 5; (Neale et al., 2010), the land module CLM4 (Community Land Model version 4 (Lawrence et al., 2011)), the ocean component POP2 (Parallel Ocean Program version 2 (Smith et al., 2010)) and the sea ice component CICE4 (Community Ice Code version 4 (Hunke et al., 2010)). The atmosphere and land components share the horizontal resolution of $1.9° \times 2.5°$ with 30 layers in the atmosphere and 15 in the land. The horizontal resolution of the ocean and sea ice is nominal $1° \times 1°$, with 60 layers in the ocean. For this model we use two transient simulations spanning the period 1501 BCE to 1850 CE branched off a equilibrium simulations for perpetual 1501 BCE

https://doi.org/10.5194/cp-2024-79
Preprint. Discussion started: 16 December 2024


Climate of the Past Discussions

conditions. The first simulation is the "orbital-only" simulation using time varying orbital parameters (Berger, 1978) and the rest of external forcing parameter set to constant 1501 BCE conditions. The second simulation is performed with all external forcings time varying, including additional greenhouse gases, total solar irradiance, land use changes and volcanic eruptions, which is the same in both models. Details on these simulations are presented in Kim et al. (2021); McConnell et al. (2020).

For all model simulations, the anomalies are calculated by subtracting the 1500 BCE to 1850 CE mean from each of the time series. Just as for the proxy reconstructions, a 100-year running mean is calculated to be able to better compare the model simulated temperatures to the glacier curves. In addition, the glacier and proxy reconstructions are compared mainly with the 'all forcing' simulations, only in the assessment for the role of internal variability vs external variability are the 'slow forcing' simulations used. The 2σ range is calculated from the standard deviation for the annual mean 100-year running mean temperatures. Anomalies for the maps are calculated by subtracting the 1500 BCE to 1850 CE mean from each time step for each grid cell. Temperatures are marked significant when the temperature value exceeds 2σ. The cold and warm periods are selected based on if they exceeded the 2σ threshold and occurred in both simulations. In addition, the minimum and maximum of the largest temperature transition are selected to visualise the maximum transitions between cold and warm periods for either model.

The volcanic radiative forcing ($W\,m^2$) is calculated by multiplying the volcanic stratospheric aerosol optical depth (SAOD) from the model output by -21 (Schmidt et al., 2018; Marshall et al., 2020). The radiative forcing for the solar irradiance was calculated by dividing the TSI by four.

3 Results and Discussion

3.1 Glacier fluctuations

Glaciers reveal the course of the climate on decadal to centurial time scales. Their mass balance reacts on the one hand to fluctuations in the radiation balance and temperature and on the other hand to the frequency of solid precipitation (Reichert et al., 2001; Steiner et al., 2008). In particular, lower summer temperatures with snowfall, which change the albedo of the glacier surface, as well as massive winter snowfalls with subsequent cold periods are of great importance. Glaciers integrate the influence of climate parameters over a longer time period. The reaction time of the individual glaciers depends heavily on their size.

The upper part of Figure 2 shows three curves with the movements of the glacier tongues of two large glaciers in the European Alps and of the largest glacier on the European mainland in Norway. The curves of the Aletsch Glacier and the Mer de Glace in the Alps show the respective position of the glacier tongue (glacial extension). As the Jostedalsbreen has the shape of an ice cap with various extensions, the fluctuations are recorded using the equilibrium line altitude (ELA).

The upper curve (burgundy) represents the sum of the combined radiative forcing (RF) from NH extra-tropical (30-90°N) volcanoes and the sun (solar irradiance). All three glacier curves show strong coherence with RF with glaciers frequently advancing during periods of strong negative forcing. This is in good agreement with analyses performed for other glaciers

https://doi.org/10.5194/cp-2024-79
Preprint. Discussion started: 16 December 2024

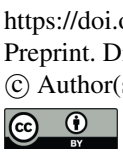

Climate of the Past Discussions

over shorter time periods (Lüthi, 2014; Sigl et al., 2018; Brönnimann et al., 2019). Overall, the curve of the ELA values of Jostedalsbreen (green curve) indicates a slower reaction. All three glaciers show a strong mass increase with advances during the 2.8 kyr event (Table 1), which has two negative RF peaks. The Jostedalsbreen reacts relatively late but very strongly during the subsequent warm period of the Roman time. The Aletsch Glacier and especially the Mer de Glace show a temporary advance after 300 CE, which is documented as a rather short-term cold relapse (Luterbacher et al., 2016). After significant glacier advances in the seventh century CE, a remarkable melting back is found during the Medieval Climate Anomaly (Table 1). Several negative peaks in the RF, which can be attributed to groups of volcanic events as well as several solar minima, are reflected in significant advances in all three glaciers during the LIA and thus to the maximum levels during the entire Neoglacial (Wanner et al., 2022).

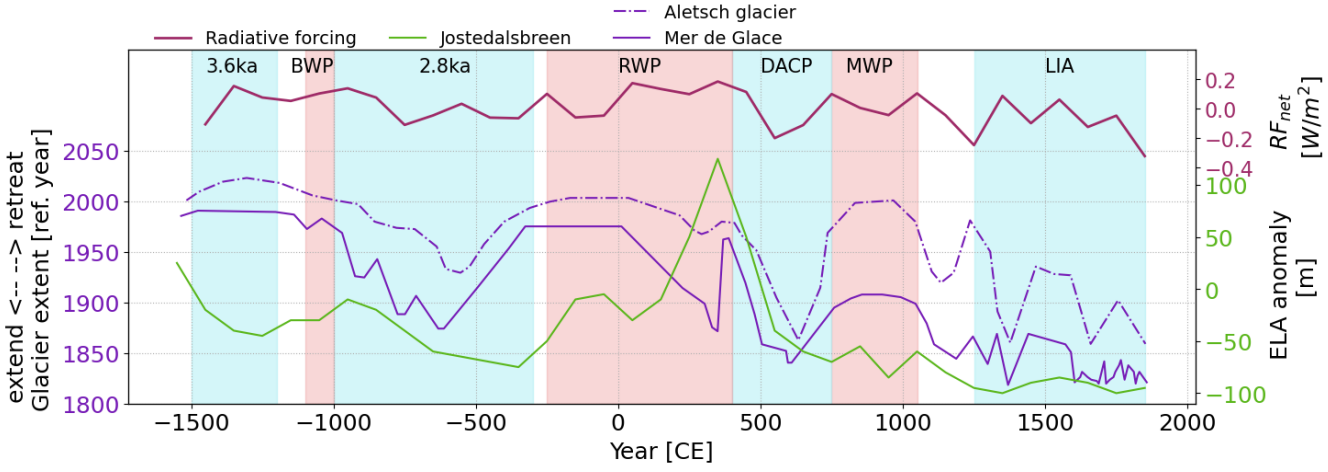

Figure 2. Glacier curves for the Aletsch glacier and the Mer de Glace in the Alps (purple) and for Jostedalsbreen in Norway (green), as well as the total net radiative forcing from solar and NH extra-tropical volcanic forcing (burgundy). The glacier extent is given compared to a reference year for the Alpine glaciers, and for the Norwegian glacier the equilibrium line altitude (ELA) anomaly is given. Cold and warm periods as defined in Table 1 are represented by the blue and red shading, respectively.

3.2 Proxy reconstructions

Unlike the glacier curves, the 100-year mean reconstructed temperature from the different proxies present a more ambiguous picture of the climate variations during the late Holocene. The cold periods appear indeed cold in some but not all proxies, and the warm periods, as defined from the glacier retreats, do not appear as particularly warm periods in the proxy reconstructions. In addition, the differences between the locations are substantial. Even proxy sites relatively close to each other, such as the tree-ring records from sites in northern Scandinavia (Fig. 3a,b, and d) show differences in centennial temperature variations. The tree-ring reconstructed temperatures from the NH (Fig. 3h) agree well with the predefined warm and cold periods, but this

https://doi.org/10.5194/cp-2024-79
Preprint. Discussion started: 16 December 2024


Climate of the Past Discussions

reconstruction only covers the Common Era.

Thus, on small spatial scales as represented by individual proxy sites, external forcing appears not to be the dominant driver of the centennial scale temperature variations over the last 3500 years. Rather, internal variability plays a more important role in the centennial changes in temperature that are recorded. A composite of several sites across a larger area, for example for the NH, results in temperature variations that agree more with the external forcing. Combining several sites dampens the signal of internal variability from each site, thereby making the forcing signal more pronounced.

3.3 Model results

For both the MPI-ESM and the CESM, boreal winter has the largest variability in temperature, and boreal summer the least (Fig. 4). This is as expected, as the winter season brings more low pressure systems over Europe, with the storm track being most strongly positioned over Northern Europe and Scandinavia. The model simulations agree more with the predefined warm and cold periods than the proxy reconstructions. However, there are discrepancies between the model simulations, and between the modeled temperature anomalies and the warm and cold periods as defined by archaeology and glacier advances.

The MPI-ESM simulates significant cooling at the predefined cold periods on a centennial scale across all of Europe, with the highest amplitude in winter (Fig. 4a,c,e). In Northern European summer, the insolation is strong, resulting in a declining trend of temperature anomalies (Fig. 4a). The Roman Warm Period is warm in the MPI-ESM simulation, whereas the Medieval Warm Period only appears warm in Northern Europe.

For the CESM, the agreement with the cold periods on the centennial scale is more elusive. The cold period around 1500-1200 BCE is cold in this model, as well as the LIA, but the two cold periods in between are not significantly cold for this model simulation, and the warm periods do not stand out either (Fig. 4b,d,f).

The largest simulated rapid temperature transition does not occur at the same time in both model simulations (Fig. 4a-b, magenta dots). For the MPI-ESM, the largest rapid transition between a centennial temperature maximum and minimum occurs during the first half of the Homeric minimum, with a cooling rate of 1.6°C per century. In the simulation from the CESM, the largest rapid transition occurs during the Roman warm period, with a cooling rate of 1.45°C per century. This indicates that the internal variability plays an important role in the simulated temperatures of the different regions in Europe.

3.3.1 Correlation with fast-varying external forcing

To test the influence of internal variability, correlations between the model simulated 100-year running mean temperatures and the 100-year running mean fast varying external forcing (combined solar and NH extra-tropical volcanic forcing) are calculated. A low correlation between the simulated 100-year mean temperature and the forcing means that the internal variability has a larger influence on the temperature fluctuations on the centennial time scale. P values are typically provided with $p<0.xx$ (in text and Table 3).

The MPI-ESM `all forcing` simulation has the highest correlation with winter temperatures for Northern Europe (r=0.50) and Central Europe (r=0.48). For summer, these correlations are slightly lower but still significant (r=0.38, p=0.05), and for

https://doi.org/10.5194/cp-2024-79
Preprint. Discussion started: 16 December 2024

Climate of the Past Discussions

Southern Europe no significant correlation with the forcing is found for either season (r=0.23 and 0.17, respectively). Surprisingly, for CESM, the highest and only significant correlations are found for Central Europe and Southern Europe during summer (r=0.36 and 0.33, respectively, p=0.05). Neither of these correlations explain more than 25% of the variance, which leads to the conclusion that the internal variability plays an important role in the temperature variations during the late Holocene when zooming in to these regions, especially in the CESM.

To study the internal variability in more detail, both model simulations are compared to their corresponding simulation without fast varying external forcing. For the MPI-ESM, this is a Holocene simulation that includes orbital forcing and greenhouse gases. For the CESM, only orbital forcing is used in the control simulation. No correlation between the slow forcing simulation and the fast varying external forcing is expected, as there is no fast varying external forcing input in these simulations. Any relatively high correlations must therefore be by chance. The MPI-ESM `orb+GHG` simulation indeed has a much lower correlation with the forcing as the `all forcing` simulation. In contrast, both CESM simulations have a similar correlation with the fast varying external forcing. Therefore, the all forcing simulation must be predominantly determined by internal variability in this model. The different correlations are presented in Table 3.

Area and Season	MPI-ESM		CESM	
	all forcing	orbital + GHG	all forcing	orbital only
Northern Europe				
DJF	**0.50**	0.24	0.13	0.14
JJA	**0.38**	0.22	0.29	**0.38**
Central Europe				
DJF	**0.48**	-0.12	0.19	0.15
JJA	**0.38**	-0.06	**0.36**	0.23
Southern Europe				
DJF	0.23	-0.07	0.20	0.18
JJA	0.17	-0.21	0.33	0.27

Table 3. Correlations between the temperature and the fast varying external forcing (combined volcanic and solar forcing) in the different simulations. Significant values (p=0.05) are in bold.

Spatial patterns

With the gridded model output, we investigate the spatial patterns of temperatures during the warm and cold periods. Two warm and two cold periods are selected for Northern Europe and Central Europe winter (DJF) for each model simulation (Fig. 4a-b and e-f, red dots). The selection is based on the periods exceeding the 2σ threshold, as well as occurring close in time in both model simulations. In figures 5 and 6, the spatial signature of these warm and cold periods for Northern Europe and Central Europe is presented. The spatial patterns for the warm (Fig. 6) and the cold (Fig. 5) periods are very similar between

https://doi.org/10.5194/cp-2024-79
Preprint. Discussion started: 16 December 2024


Climate of the Past Discussions

the MPI-ESM and CESM. This is especially true for cold and warm periods in Northern Europe, where all of the chosen time frames exhibit similar patterns in both models, with the main center of cooling around Northern Scandinavia and the Barents Sea. Studying the temperature anomaly patterns for the entire NH (not shown here), three out of the four periods also indicate similar patterns on a hemispheric scale. For Central Europe, only the cold periods exhibit similar patterns on a continental scale (Fig. 5 e-h), with again the center of the cooling around the Barent Sea, as well as over central Europe. The mid-sixth century, as well as the late 15th century both indicate similar temperature anomaly patterns also on a hemispheric scale. For the warm period around the 13th century, both MPI and CESM simulate a similar warming anomaly over central Europe. However, for the warm period around 0 CE, the spatial temperature patterns exhibit slight differences on a continental scale (Fig. 6 f,g), with MPI simulating warm anomalies over central Europe, whereas CESM simulates the main warm anomalies over northern Europe. This is exacerbated on the hemispheric scale.

For Northern and Central Europe, the cold periods display roughly the same anomaly patterns for both models. This indicates that the cold periods are possibly more affected by the integrated (predominantly volcanic) external forcing, peaking at slightly different years owing to slightly different response mechanisms in each model. For example, this could be due to the ocean-sea ice feedback that sets in after the initial direct cooling from the forcing (Lehner et al., 2013). In both models, the main cold anomalies are present over the Barents Sea, which is an important area for sea ice formation. In contrast, the warm periods exhibit fewer similarities in patterns between the models, indicating a larger influence of internal variability for these periods.

4 Conclusions

The late Holocene shows pronounced cold and warm periods, as defined by the literature (Table 1). These definitions often stem from archaeology, or from glacier advances in the Alps and Scandinavia and are widely used in especially the archaeology to link climatic changes to changes in societies. However, glacier advances are often the result of the integrated effect of temperature changes over a longer time, thereby smoothing the temperature signal. While the glacier advances as reconstructed for the late Holocene agree very well with the smoothed mean for fast varying external forcing of solar radiation changes and volcanic eruptions, this does not capture all the nuances of the highly varying climate on annual to decadal scale. In contrast, high-resolution paleo-proxy reconstructions from tree-rings and speleothems indicate that the local sites at which the temperature changes are recorded, are dominated by internal variability, masking to some extent the signal of external forcing on the centennial scale. Climate model simulations also indicate a greater influence of internal variability for smaller areas. In the MPI model, Northern Europe is influenced more by external forcing than Central Europe and Southern Europe, with the latter being very insensitive to external fast varying external forcing in these simulations. This could be due to possible sea-ice feedback mechanisms (Lehner et al., 2013). However, in CESM the results are rather ambiguous, which shows that sensitivity to external forcing is also part of model uncertainty. Centennial cold periods are more likely to be the result of changes in external forcing, as the temperature anomaly patterns for the selected cold periods are the same for both the MPI-ESM and the CESM. On the other hand, warm periods appear to be less sensitive to external fast varying external forcing, indicated by

https://doi.org/10.5194/cp-2024-79
Preprint. Discussion started: 16 December 2024

the variety of temperature anomaly patterns between the models, as well as between the different warm periods in each model simulation.

Thus, warm and cold periods in the late Holocene did occur, but caution is needed when interpreting events or results encompassing a small area. The cold and warm periods in the last 4000 years are not homogeneously distributed over Europe, and for local sites internal variability is on the same order of magnitude (or larger) as the effect of fast varying external forcing, making comparison between different locations for a certain warm or cold period challenging.

Code and data availability. The CESM data is archived and accessible via (doi). MPI data is available on Zenodo (https://doi.org/10.5281/zenodo.10409454). Code is available on github (https://github.com/EvelienvanDijk/late-Holocene)

Author contributions. EvD, CCR, MS, and HW developed the idea and the framework for the paper. JJ and CCR carried out the model simulations. EvD processed the data, performed the analysis, and designed the figures. HW, MS, and CCR contributed to the interpretation of the results. All authors discussed the results and helped writing the manuscript.

Competing interests. The authors declare no competing interests.

Acknowledgements. CCR acknowledge the Swiss National Supercomputing Centre (CSCS) in Lugano, Switzerland, for providing the necessary computational resources and supercomputing architecture. CCR received funding from the Swiss National Science Foundation (grant nos. 200020_172745 and IZCOZ0_205416). The authors would like to thank Hanspeter Holzhauser and Atle Nesje for the data sets and the graphical overviews of the Aletsch Glacier and the Jostedalsbreen. EvD and MS acknowledge the support of the ERC under the European Union's Horizon 2020 research and innovation program (grant agreement 820047).

https://doi.org/10.5194/cp-2024-79
Preprint. Discussion started: 16 December 2024

Climate of the Past Discussions

References

Affolter, S., Häuselmann, A., Fleitmann, D., Edwards, R. L., Cheng, H., and Leuenberger, M.: Central Europe temperature constrained by speleothem fluid inclusion water isotopes over the past 14,000 years, Science advances, 5, eaav3809, 2019.

Bader, J., Jungclaus, J., Krivova, N., Lorenz, S., Maycock, A., Raddatz, T., Schmidt, H., Toohey, M., Wu, C.-J., and Claussen, M.: Global temperature modes shed light on the Holocene temperature conundrum, Nature communications, 11, 1–8, 2020.

Baker, J. L., Lachniet, M. S., Chervyatsova, O., Asmerom, Y., and Polyak, V. J.: Holocene warming in western continental Eurasia driven by glacial retreat and greenhouse forcing, Nature Geoscience, 10, 430–435, 2017.

Berger, A. L.: Long-Term Variations of Caloric Insolation Resulting from the Earth's Orbital Elements 1, Quaternary research, 9, 139–167, 1978.

Bernard, S., McConnell, J., Di Rita, F., Michelangeli, F., Magri, D., Sadori, L., Masi, A., Zanchetta, G., Bini, M., Celant, A., et al.: An Environmental and Climate History of the Roman Expansion in Italy, The Journal of Interdisciplinary History, 54, 1–41, 2023.

Bova, S., Rosenthal, Y., Liu, Z., Godad, S. P., and Yan, M.: Seasonal origin of the thermal maxima at the Holocene and the last interglacial, Nature, 589, 548–553, 2021.

Boxleitner, M., Ivy-Ochs, S., Egli, M., Brandova, D., Christl, M., Dahms, D., and Maisch, M.: The 10Be deglaciation chronology of the Göschenertal, central Swiss Alps, and new insights into the Göschenen Cold Phases, Boreas, 48, 867–878, 2019.

Bradley, R. S. and Bakke, J.: Is there evidence for a 4.2 ka BP event in the northern North Atlantic region?, Climate of the Past, 15, 1665–1676, 2019.

Bradley, R. S., Hughes, M. K., and Diaz, H. F.: Climate in medieval time, Science, 302, 404–405, 2003.

Bradley, R. S., Wanner, H., and Diaz, H. F.: The medieval quiet period, The Holocene, 26, 990–993, 2016.

Brönnimann, S., Franke, J., Nussbaumer, S. U., Zumbühl, H. J., Steiner, D., Trachsel, M., Hegerl, G. C., Schurer, A., Worni, M., Malik, A., et al.: Last phase of the Little Ice Age forced by volcanic eruptions, Nature geoscience, 12, 650–656, 2019.

Brovkin, V., Lorenz, S., Raddatz, T., Ilyina, T., Stemmler, I., Toohey, M., and Claussen, M.: What was the source of the atmospheric CO_2 increase during the Holocene?, Biogeosciences, 16, 2543–2555, 2019.

Büntgen, U., Tegel, W., Nicolussi, K., McCormick, M., Frank, D., Trouet, V., Kaplan, J. O., Herzig, F., Heussner, K.-U., Wanner, H., et al.: 2500 years of European climate variability and human susceptibility, science, 331, 578–582, 2011.

Büntgen, U., Myglan, V. S., Ljungqvist, F. C., McCormick, M., Di Cosmo, N., Sigl, M., Jungclaus, J., Wagner, S., Krusic, P. J., Esper, J., et al.: Cooling and societal change during the Late Antique Little Ice Age from 536 to around 660 AD, Nature Geoscience, 9, 231, 2016.

Büntgen, U., Allen, K., Anchukaitis, K. J., Arseneault, D., Boucher, É., Bräuning, A., Chatterjee, S., Cherubini, P., Churakova, O. V., Corona, C., et al.: The influence of decision-making in tree ring-based climate reconstructions, Nature communications, 12, 3411, 2021.

Cartapanis, O., Jonkers, L., Moffa-Sanchez, P., Jaccard, S. L., and de Vernal, A.: Complex spatio-temporal structure of the Holocene Thermal Maximum, nature communications, 13, 5662, 2022.

Charpentier Ljungqvist, F.: The spatio-temporal pattern of the mid-Holocene thermal maximum, Geografie–Sborník ČGS, 116, 91–110, 2011.

Dallmeyer, A., Claussen, M., Lorenz, S. J., Sigl, M., Toohey, M., and Herzschuh, U.: Holocene vegetation transitions and their climatic drivers in MPI-ESM1. 2, Climate of the Past, 17, 2481–2513, 2021.

Diaz, H. F., Trigo, R., Hughes, M. K., Mann, M. E., Xoplaki, E., and Barriopedro, D.: Spatial and temporal characteristics of climate in medieval times revisited, Bulletin of the American Meteorological Society, 92, 1487–1500, 2011.

https://doi.org/10.5194/cp-2024-79
Preprint. Discussion started: 16 December 2024

Essell, H., Krusic, P. J., Esper, J., Wagner, S., Braconnot, P., Jungclaus, J., Muschitiello, F., Oppenheimer, C., and Büntgen, U.: A frequency-optimised temperature record for the Holocene, Environmental Research Letters, 18, 114 022, 2023.

Fohlmeister, J., Schröder-Ritzrau, A., Scholz, D., Spötl, C., Riechelmann, D. F., Mudelsee, M., Wackerbarth, A., Gerdes, A., Riechelmann, S., Immenhauser, A., et al.: Bunker Cave stalagmites: an archive for central European Holocene climate variability, Climate of the Past, 8, 1751–1764, 2012.

Gabriel, I., Plunkett, G., Abbott, P. M., Behrens, M., Burke, A., Chellman, N., Cook, E., Fleitmann, D., Hörhold, M., Hutchison, W., et al.: Decadal-to-centennial increases of volcanic aerosols from Iceland challenge the concept of a Medieval Quiet Period, Communications earth & environment, 5, 194, 2024.

Grove, J. M.: Little Ice Ages. Ancient and modern, Methuen, London, 1988.

Grudd, H., Briffa, K. R., Karlén, W., Bartholin, T. S., Jones, P. D., and Kromer, B.: A 7400-year tree-ring chronology in northern Swedish Lapland: natural climatic variability expressed on annual to millennial timescales, The Holocene, 12, 657–665, 2002.

Haldon, J.: Cooling and societal change, Nature Geoscience, 9, 191–192, 2016.

Haldon, J., Mordechai, L., Newfield, T. P., Chase, A. F., Izdebski, A., Guzowski, P., Labuhn, I., and Roberts, N.: History meets palaeoscience: Consilience and collaboration in studying past societal responses to environmental change, Proceedings of the National Academy of Sciences, 115, 3210–3218, 2018.

Hantemirov, R., Gorlanova, L., Bessonova, V., Hamzin, I., and Kukarskih, V.: A 4500-Year Tree-Ring Record of Extreme Climatic Events on the Yamal Peninsula, Forests, 14, 574, 2023.

Heikkilä, M. and Seppä, H.: A 11,000 yr palaeotemperature reconstruction from the southern boreal zone in Finland, Quaternary Science Reviews, 22, 541–554, 2003.

Helama, S., Läänelaid, A., Tietäväinen, H., Fauria, M. M., Kukkonen, I. T., Holopainen, J., Nielsen, J. K., and Valovirta, I.: Late Holocene climatic variability reconstructed from incremental data from pines and pearl mussels–a multi-proxy comparison of air and subsurface temperatures, Boreas, 39, 734–748, 2010.

Helama, S., Jones, P. D., and Briffa, K. R.: Dark Ages Cold Period: A literature review and directions for future research, The Holocene, 27, 1600–1606, 2017.

Helama, S., Herva, H., Arppe, L., Gunnarson, B., Frank, T., Holopainen, J., Nöjd, P., Mäkinen, H., Mielikäinen, K., Sutinen, R., et al.: Disentangling the Evidence of Milankovitch Forcing From Tree-Ring and Sedimentary Records, Frontiers in Earth Science, 10, 871 641, 2022.

Holzhauser, H., Magny, M., and Zumbuühl, H. J.: Glacier and lake-level variations in west-central Europe over the last 3500 years, The Holocene, 15, 789–801, 2005.

Hopcroft, P. O., Valdes, P. J., Shuman, B. N., Toohey, M., and Sigl, M.: Relative importance of forcings and feedbacks in the Holocene temperature conundrum, Quaternary Science Reviews, 319, 108 322, 2023.

Hughes, M. K. and Diaz, H. F.: Was there a 'Medieval Warm Period', and if so, where and when?, Climatic change, 26, 109–142, 1994.

Hunke, E. C., Lipscomb, W. H., Turner, A. K., Jeffery, N., and Elliott, S.: Cice: the los alamos sea ice model documentation and software user's manual version 4.1 la-cc-06-012, T-3 Fluid Dynamics Group, Los Alamos National Laboratory, 675, 500, 2010.

Hurrell, J. W., Holland, M. M., Gent, P. R., Ghan, S., Kay, J. E., Kushner, P. J., Lamarque, J.-F., Large, W. G., Lawrence, D., Lindsay, K., Lipscomb, W. H., Long, M. C., Mahowald, N., Marsh, D. R., Neale, R. B., Rasch, P., Vavrus, S., Vertenstein, M., Bader, D., Collins, W. D., Hack, J. J., Kiehl, J., and Marshall, S.: The community earth system model: a framework for collaborative research, Bulletin of the American Meteorological Society, 94, 1339–1360, https://doi.org/10.1175/BAMS-D-12-00121.1, 2013.

https://doi.org/10.5194/cp-2024-79
Preprint. Discussion started: 16 December 2024

Hurtt, G. C., Chini, L., Sahajpal, R., Frolking, S., Bodirsky, B. L., Calvin, K., Doelman, J. C., Fisk, J., Fujimori, S., Klein Goldewijk, K., et al.: Harmonization of global land use change and management for the period 850–2100 (LUH2) for CMIP6, Geoscientific Model Development, 13, 5425–5464, 2020.

Jalali, B. and Sicre, M.-A.: The 4.2 ka event in the Euro-Mediterranean region—a study from the MISTRALS/PALEOMEX program, in: Patterns and Mechanisms of Climate, Paleoclimate and Paleoenvironmental Changes from Low-Latitude Regions: Proceedings of the 1st Springer Conference of the Arabian Journal of Geosciences (CAJG-1), Tunisia 2018, pp. 13–15, Springer, 2019.

Jørgensen, E. K. and Riede, F.: Convergent catastrophes and the termination of the Arctic Norwegian Stone Age: A multi-proxy assessment of the demographic and adaptive responses of mid-Holocene collectors to biophysical forcing, The Holocene, 29, 1782–1800, 2019.

Jouvet, G. and Huss, M.: Future retreat of great Aletsch glacier, Journal of Glaciology, 65, 869–872, 2019.

Jungclaus, J., Fischer, N., Haak, H., Lohmann, K., Marotzke, J., Matei, D., Mikolajewicz, U., Notz, D., and Von Storch, J.: Characteristics of the ocean simulations in the Max Planck Institute Ocean Model (MPIOM) the ocean component of the MPI-Earth system model, Journal of Advances in Modeling Earth Systems, 5, 422–446, 2013.

Kaufman, D., McKay, N., Routson, C., Erb, M., Dätwyler, C., Sommer, P. S., Heiri, O., and Davis, B.: Holocene global mean surface temperature, a multi-method reconstruction approach, Scientific data, 7, 1–13, 2020.

Kaufman, D. S. and Broadman, E.: Revisiting the Holocene global temperature conundrum, Nature, 614, 425–435, 2023.

Kaufman, D. S., Ager, T. A., Anderson, N. J., Anderson, P. M., Andrews, J. T., Bartlein, P. J., Brubaker, L. B., Coats, L. L., Cwynar, L. C., Duvall, M. L., et al.: Holocene thermal maximum in the western Arctic (0–180 W), Quaternary Science Reviews, 23, 529–560, 2004.

Kim, W. M., Blender, R., Sigl, M., Messmer, M., and Raible, C. C.: Statistical characteristics of extreme daily precipitation during 1501 BCE-1849 CE in the Community Earth System Model, Climate of the Past, 17, 2031–2053, https://doi.org/10.5194/cp-17-2031-2021, 2021.

Köhler, P.: Interactive comment on "What was the source of the atmospheric CO_2 increase during the Holocene?" by Victor Brovkin et al., Biogeosciences Discussions, 16, SC1, 2019.

Krivova, N., Solanki, S., and Unruh, Y.: Towards a long-term record of solar total and spectral irradiance, Journal of Atmospheric and Solar-Terrestrial Physics, 73, 223–234, 2011.

Lamb, H. H.: The early medieval warm epoch and its sequel, Palaeogeography, Palaeoclimatology, Palaeoecology, 1, 13–37, 1965.

Lawrence, D. M., Oleson, K. W., Flanner, M. G., Thornton, P. E., Swenson, S. C., Lawrence, P. J., Zeng, X., Yang, Z.-L., Levis, S., Sakaguchi, K., Bonan, G. B., and Slater, A. G.: Parameterization improvements and functional and structural advances in version 4 of the Community Land Model, Journal of Advances in Modeling Earth Systems, 3, https://doi.org/10.1029/2011MS00045, 2011.

Le Roy, M., Nicolussi, K., Deline, P., Astrade, L., Edouard, J.-L., Miramont, C., and Arnaud, F.: Calendar-dated glacier variations in the western European Alps during the Neoglacial: the Mer de Glace record, Mont Blanc massif, Quaternary Science Reviews, 108, 1–22, 2015.

Lehner, F., Born, A., Raible, C. C., and Stocker, T. F.: Amplified inception of European Little Ice Age by sea ice–ocean–atmosphere feedbacks, Journal of climate, 26, 7586–7602, 2013.

Liu, Z., Zhu, J., Rosenthal, Y., Zhang, X., Otto-Bliesner, B. L., Timmermann, A., Smith, R. S., Lohmann, G., Zheng, W., and Elison Timm, O.: The Holocene temperature conundrum, Proceedings of the National Academy of Sciences, 111, E3501–E3505, 2014.

Luterbacher, J., Werner, J. P., Smerdon, J. E., Fernández-Donado, L., González-Rouco, F. J., Barriopedro, D., Ljungqvist, F. C., Büntgen, U., Zorita, E., Wagner, S., et al.: European summer temperatures since Roman times, Environmental research letters, 11, 024 001, 2016.

https://doi.org/10.5194/cp-2024-79
Preprint. Discussion started: 16 December 2024

Lüthi, M. P.: Little Ice Age climate reconstruction from ensemble reanalysis of Alpine glacier fluctuations, The Cryosphere, 8, 639–650, 2014.

Mann, M. E.: Little ice age, Encyclopedia of global environmental change, 1, 504–509, 2002.

Manning, J. G., Ludlow, F., Stine, A. R., Boos, W. R., Sigl, M., and Marlon, J. R.: Volcanic suppression of Nile summer flooding triggers revolt and constrains interstate conflict in ancient Egypt, Nature communications, 8, 900, 2017.

Manning, K. and Timpson, A.: The demographic response to Holocene climate change in the Sahara, Quaternary Science Reviews, 101, 28–35, 2014.

Marcott, S. A., Shakun, J. D., Clark, P. U., and Mix, A. C.: A reconstruction of regional and global temperature for the past 11,300 years, Science, 339, 1198–1201, 2013.

Margaritelli, G., Cacho, I., Català, A., Barra, M., Bellucci, L., Lubritto, C., Rettori, R., and Lirer, F.: Persistent warm Mediterranean surface waters during the Roman period, Scientific Reports, 10, 10 431, 2020.

Marshall, L. R., Smith, C. J., Forster, P. M., Aubry, T. J., Andrews, T., and Schmidt, A.: Large variations in volcanic aerosol forcing efficiency due to eruption source parameters and rapid adjustments, Geophysical Research Letters, 47, e2020GL090 241, 2020.

Marsicek, J., Shuman, B. N., Bartlein, P. J., Shafer, S. L., and Brewer, S.: Reconciling divergent trends and millennial variations in Holocene temperatures, Nature, 554, 92–96, 2018.

Martín-Chivelet, J., Muñoz-García, M. B., Edwards, R. L., Turrero, M. J., and Ortega, A. I.: Land surface temperature changes in Northern Iberia since 4000 yr BP, based on δ13C of speleothems, Global and Planetary Change, 77, 1–12, 2011.

Martin-Puertas, C., Matthes, K., Brauer, A., Muscheler, R., Hansen, F., Petrick, C., Aldahan, A., Possnert, G., and Van Geel, B.: Regional atmospheric circulation shifts induced by a grand solar minimum, Nature Geoscience, 5, 397–401, 2012.

Matthes, F. E.: Report of committee on glaciers, April 1939, Eos, Transactions American Geophysical Union, 20, 518–523, 1939.

Matthews, J. A. and Briffa, K. R.: The 'Little Ice Age': re-evaluation of an evolving concept, Geografiska Annaler: Series A, Physical Geography, 87, 17–36, 2005.

Mauritsen, T., Bader, J., Becker, T., Behrens, J., Bittner, M., Brokopf, R., Brovkin, V., Claussen, M., Crueger, T., Esch, M., et al.: Developments in the MPI-M Earth System Model version 1.2 (MPI-ESM1. 2) and Its Response to Increasing CO2, Journal of Advances in Modeling Earth Systems, 11, 998–1038, 2019.

Mayewski, P. A., Rohling, E. E., Stager, J. C., Karlén, W., Maasch, K. A., Meeker, L. D., Meyerson, E. A., Gasse, F., van Kreveld, S., Holmgren, K., et al.: Holocene climate variability, Quaternary research, 62, 243–255, 2004.

McConnell, J. R., Sigl, M., Plunkett, G., Burke, A., Kim, W. M., Raible, C. C., Wilson, I, A., Manning, J. G., Ludlow, F., Chellman, N. J., Innes, H. M., Yang, Z., Larsen, J. F., Schaefer, J. R., Kipfstuhl, S., Mojtabavi, S., Wilhelms, F., Opel, T., Meyer, H., and Steffensen, J. P.: Extreme climate after massive eruption of Alaska's Okmok volcano in 43 BCE and effects on the late Roman Republic and Ptolemaic Kingdom, Proceedings of the National Academy of Sciences of the United States of America, 117, 15 443–15 449, https://doi.org/10.1073/pnas.2002722117, 2020.

McCormick, M., Dutton, P. E., and Mayewski, P. A.: Volcanoes and the climate forcing of Carolingian Europe, AD 750-950, Speculum, 82, 865–895, 2007.

McCormick, M., Büntgen, U., Cane, M. A., Cook, E. R., Harper, K., Huybers, P., Litt, T., Manning, S. W., Mayewski, P. A., More, A. F., et al.: Climate change during and after the Roman Empire: reconstructing the past from scientific and historical evidence, Journal of Interdisciplinary History, 43, 169–220, 2012.

https://doi.org/10.5194/cp-2024-79
Preprint. Discussion started: 16 December 2024

McKay, N. P., Kaufman, D. S., Arcusa, S. H., Kolus, H. R., Edge, D. C., Erb, M. P., Hancock, C. L., Routson, C. C., Żarczyński, M., Marshall, L. P., et al.: The 4.2 ka event is not remarkable in the context of Holocene climate variability, Nature Communications, 15, 6555, 2024.

Moran, A. P., Ivy Ochs, S., Christl, M., and Kerschner, H.: Exposure dating of a pronounced glacier advance at the onset of the late-Holocene in the central Tyrolean Alps, The Holocene, 27, 1350–1358, 2017.

Neale, R. B., Chen, C.-C., Gettelman, A., Lauritzen, P. H., Park, S., Williamson, D. L., Conley, A. J., Garcia, R., Kinnison, D., and Lamarque, J.-F.: Description of the NCAR community atmosphere model (CAM 5.0), NCAR Tech. Note NCAR/TN-486+ STR, 1, 1–12, 2010.

Nesje, A.: Latest Pleistocene and Holocene alpine glacier fluctuations in Scandinavia, Quaternary Science Reviews, 28, 2119–2136, 2009.

Nesje, A., Dahl, S. O., Andersson, C., and Matthews, J. A.: The lacustrine sedimentary sequence in Sygneskardvatnet, western Norway: a continuous, high-resolution record of the Jostedalsbreen ice cap during the Holocene, Quaternary Science Reviews, 19, 1047–1065, 2000.

Nesje, A., Matthews, J. A., Dahl, S. O., Berrisford, M. S., and Andersson, C.: Holocene glacier fluctuations of Flatebreen and winter-precipitation changes in the Jostedalsbreen region, western Norvay, based on glaciolacustrine sediment records, The Holocene, 11, 267–280, 2001.

Oerlemans, J.: Extracting a climate signal from 169 glacier records, science, 308, 675–677, 2005.

Palacios, D., Hughes, P. D., Jomelli, V., and Tanarro, L. M.: European Glacial Landscapes: The Holocene, Elsevier, 2023.

Patzelt, G. and Bortenschlager, S.: Die postglazialen Gletscher-und Klimaschwankungen in der Venedigergruppe (Hohe Tauern, Ostalpen), Zeitschrift fur Geomorphologie NF Supplement 9, 5-57, 1973.

Pearson, C., Sigl, M., Burke, A., Davies, S., Kurbatov, A., Severi, M., Cole-Dai, J., Innes, H., Albert, P. G., and Helmick, M.: Geochemical ice-core constraints on the timing and climatic impact of Aniakchak II (1628 BCE) and Thera (Minoan) volcanic eruptions, PNAS nexus, 1, pgac048, 2022.

Porter, S. C. and Denton, G. H.: Chronology of neoglaciation in the North American Cordillera, American Journal of Science, 265, 177–210, 1967.

Reichert, B. K., Bengtsson, L., and Oerlemans, J.: Midlatitude forcing mechanisms for glacier mass balance investigated using general circulation models, Journal of Climate, 14, 3767–3784, 2001.

Renssen, H., Seppä, H., Crosta, X., Goosse, H., and Roche, D. M.: Global characterization of the Holocene thermal maximum, Quaternary Science Reviews, 48, 7–19, 2012.

Roland, T. P., Caseldine, C. J., Charman, D. J., Turney, C. S., and Amesbury, M. J.: Was there a '4.2 ka event'in Great Britain and Ireland? Evidence from the peatland record, Quaternary Science Reviews, 83, 11–27, 2014.

Schmidt, A., Mills, M. J., Ghan, S., Gregory, J. M., Allan, R. P., Andrews, T., Bardeen, C. G., Conley, A., Forster, P. M., Gettelman, A., et al.: Volcanic radiative forcing from 1979 to 2015, Journal of Geophysical Research: Atmospheres, 123, 12 491–12 508, 2018.

Sigl, M., Winstrup, M., McConnell, J. R., Welten, K. C., Plunkett, G., Ludlow, F., Büntgen, U., Caffee, M., Chellman, N., Dahl-Jensen, D., et al.: Timing and climate forcing of volcanic eruptions for the past 2,500 years, Nature, 523, 543–549, 2015.

Sigl, M., Abram, N. J., Gabrieli, J., Jenk, T. M., Osmont, D., and Schwikowski, M.: 19th century glacier retreat in the Alps preceded the emergence of industrial black carbon deposition on high-alpine glaciers, The Cryosphere, 12, 3311–3331, 2018.

Sigl, M., Toohey, M., McConnell, J. R., Cole-Dai, J., and Severi, M.: Volcanic stratospheric sulfur injections and aerosol optical depth during the Holocene (past 11 500 years) from a bipolar ice-core array, Earth System Science Data, 14, 3167–3196, 2022.

Smith, R., Jones, P., Briegleb, B., Bryan, F., Danabasoglu, G., Dennis, J., Dukowicz, J., Eden, C., Fox-Kemper, B., Gent, P., Hecht, M., Jayne, S., Jochum, M., Large, W., Lindsay, K., Maltrud, M., Norton, N., Peacock, S., Vertenstein, M., and Yeager, S.: The parallel ocean

https://doi.org/10.5194/cp-2024-79
Preprint. Discussion started: 16 December 2024

program (POP) reference manual ocean component of the community climate system model (CCSM) and community earth system model (CESM), LAUR-01853, 141, 1–140, 2010.

Solomina, O. N., Bradley, R. S., Hodgson, D. A., Ivy-Ochs, S., Jomelli, V., Mackintosh, A. N., Nesje, A., Owen, L. A., Wanner, H., Wiles, G. C., et al.: Holocene glacier fluctuations, Quaternary Science Reviews, 111, 9–34, 2015.

Staubwasser, M. and Weiss, H.: Holocene climate and cultural evolution in late prehistoric–early historic West Asia, Quaternary Research, 66, 372–387, 2006.

Steiner, D., Pauling, A., Nussbaumer, S. U., Nesje, A., Luterbacher, J., Wanner, H., and Zumbühl, H. J.: Sensitivity of European glaciers to precipitation and temperature–two case studies, Climatic Change, 90, 413–441, 2008.

Stevens, B., Giorgetta, M., Esch, M., Mauritsen, T., Crueger, T., Rast, S., Salzmann, M., Schmidt, H., Bader, J., Block, K., et al.: Atmospheric component of the MPI-M Earth system model: ECHAM6, Journal of Advances in Modeling Earth Systems, 5, 146–172, 2013.

Tian, Z., Jiang, D., Zhang, R., and Su, B.: Transient climate simulations of the Holocene (version 1)–experimental design and boundary conditions, Geoscientific Model Development, 15, 4469–4487, 2022.

Toohey, M., Krüger, K., Sigl, M., Stordal, F., and Svensen, H.: Climatic and societal impacts of a volcanic double event at the dawn of the Middle Ages, Climatic Change, 136, 401–412, 2016.

Van Dijk, E., Jungclaus, J., Lorenz, S., Timmreck, C., and Krüger, K.: Was there a volcanic-induced long-lasting cooling over the Northern Hemisphere in the mid-6th–7th century?, Climate of the Past, 18, 1601–1623, 2022.

van Dijk, E. J., Jungclaus, J., Sigl, M., Timmreck, C., and Krüger, K.: High-frequency climate forcing causes prolonged cold periods in the Holocene, Communications Earth & Environment, 5, 242, 2024.

Vasskog, K., Paasche, Ø., Nesje, A., Boyle, J. F., and Birks, H.: A new approach for reconstructing glacier variability based on lake sediments recording input from more than one glacier, Quaternary Research, 77, 192–204, 2012.

Walker, M. J., Berkelhammer, M., Björck, S., Cwynar, L. C., Fisher, D. A., Long, A. J., Lowe, J. J., Newnham, R. M., Rasmussen, S. O., and Weiss, H.: Formal subdivision of the Holocene Series/Epoch: a Discussion Paper by a Working Group of INTIMATE (Integration of ice-core, marine and terrestrial records) and the Subcommission on Quaternary Stratigraphy (International Commission on Stratigraphy), Journal of Quaternary Science, 27, 649–659, 2012.

Wanner, H.: Late-Holocene: cooler or warmer?, The Holocene, 31, 1501–1506, 2021.

Wanner, H., Pfister, C., and Neukom, R.: The variable European Little Ice Age, Quaternary science reviews, 287, 107 531, 2022.

Weiss, H. and Bradley, R. S.: What drives societal collapse?, Science, 291, 609–610, 2001.

Weldeab, S., Menke, V., and Schmiedl, G.: The pace of East African monsoon evolution during the Holocene, Geophysical Research Letters, 41, 1724–1732, 2014.

Zoller, H.: Postglaziale Gletscherstände und Klimaschwankungen im Gotthardmassiv und Vorderrheingebiet, Verlag nicht ermittelbar, 1966.

https://doi.org/10.5194/cp-2024-79
Preprint. Discussion started: 16 December 2024

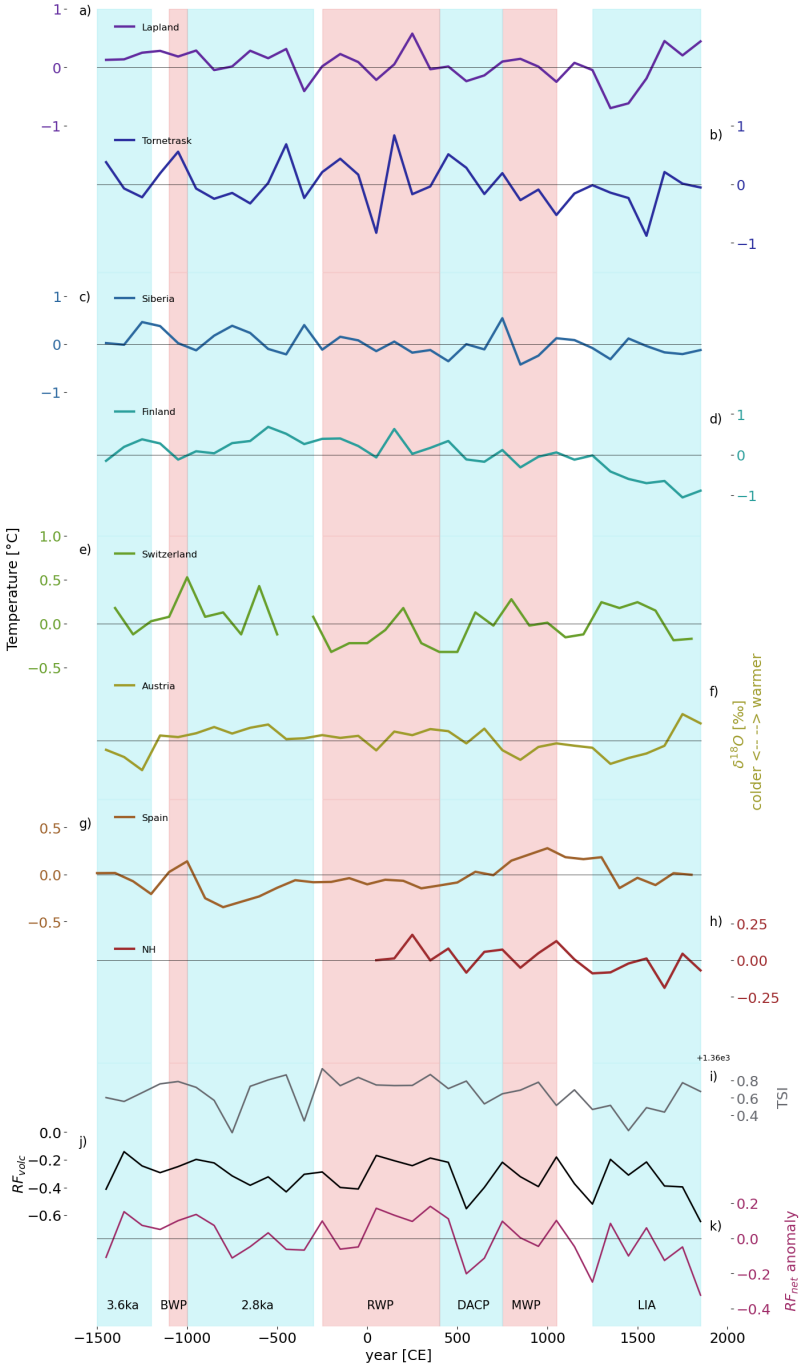

Figure 3. 100-year mean climate reconstruction for a) Lapland (tree-ring width) (Helama et al., 2010), b) Tornetrask (tree-ring width) (Grudd et al., 2002), c) Siberia (tree-ring anatomy) (Hantemirov et al., 2023), d) Finland (tree-ring) (Helama et al., 2022), e) Switzerland (speleothems) (Affolter et al., 2019), f) Austria (speleothems) (Fohlmeister et al., 2012), g) Spain (speleothems) (Martín-Chivelet et al., 2011), h) NH (tree-ring width) (Büntgen et al., 2021), i) solar forcing (TSI) (Krivova et al., 2011), j) NH extra-tropical volcanic forcing (Sigl et al., 2022), and k) solar and volcanic forcing combined. Cold and warm periods are represented by the blue and red shading, respectively, based on glacier advances and archaeological definitions (Table 1).

https://doi.org/10.5194/cp-2024-79
Preprint. Discussion started: 16 December 2024

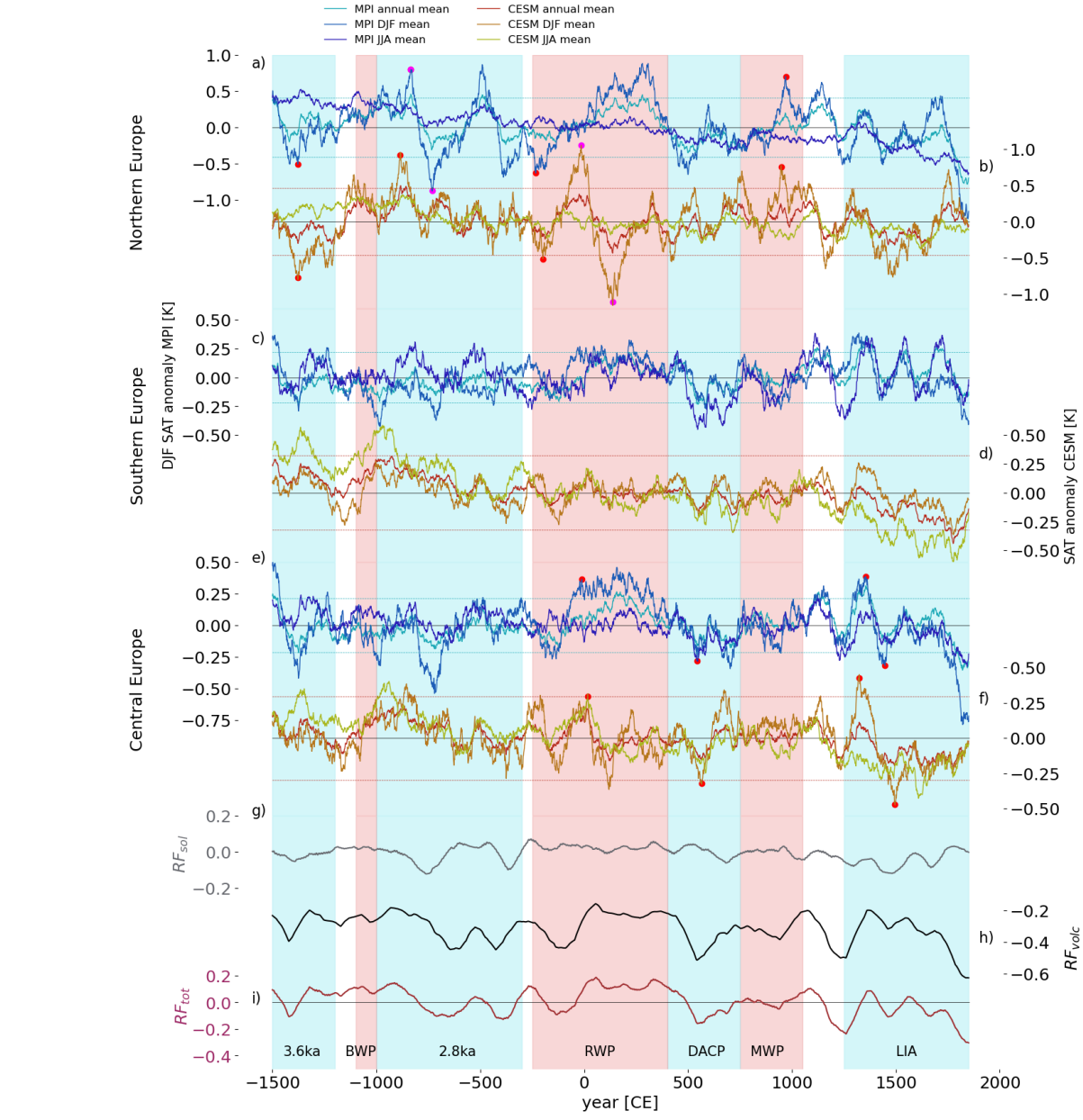

Figure 4. 100-year running mean, annual, boreal winter (DJF), and boreal summer (JJA) simulated temperature anomalies for Northern Europe a) MPI, b) CESM, Southern Europe c) MPI, d) CESM, and Central Europe e) MPI, f) CESM, as well as the g) solar forcing (TSI) (Krivova et al., 2011), h) NH extra-tropical (30-90N) volcanic forcing (Sigl et al., 2022), and i) solar and volcanic forcing combined. 2σ for the annual mean is represented by the dashed horizontal lines. Cold and warm periods are represented by the blue and red shading, respectively, based on glacier advances and archaeological definitions (Table 1). Red dots represent the cold and warm periods taken for spatial comparison, and the magenta dots represent the minimum and maximum taken for the maximum temperature transition.

https://doi.org/10.5194/cp-2024-79
Preprint. Discussion started: 16 December 2024

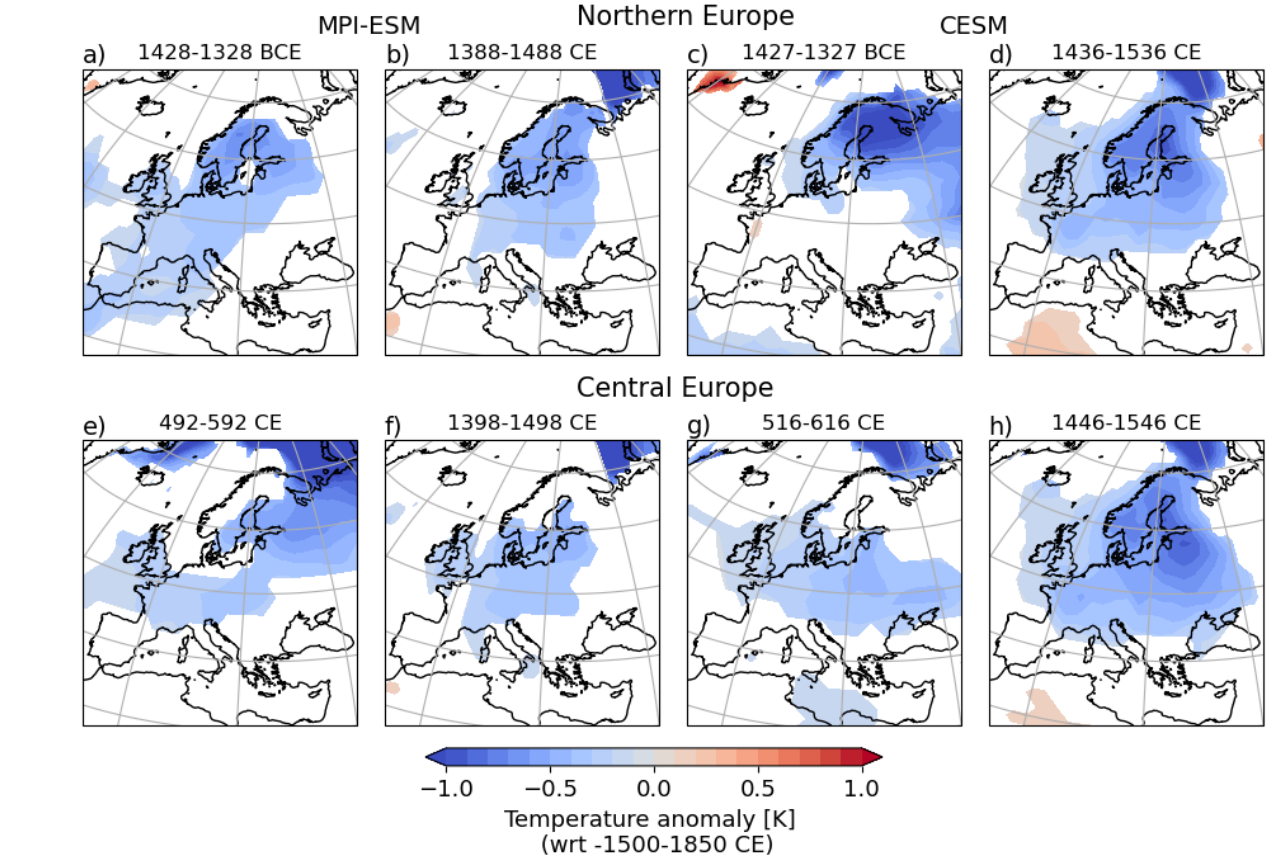

Figure 5. Spatial comparison for selected 100-year cold periods (mean) in MPI (a,b,e,f) and CESM (c,d,g,h) for Northern Europe (a-d) and Central Europe (e-h). Temperature anomalies are with respect to the 1500 BCE - 1850 CE mean from the control simulations.

https://doi.org/10.5194/cp-2024-79
Preprint. Discussion started: 16 December 2024

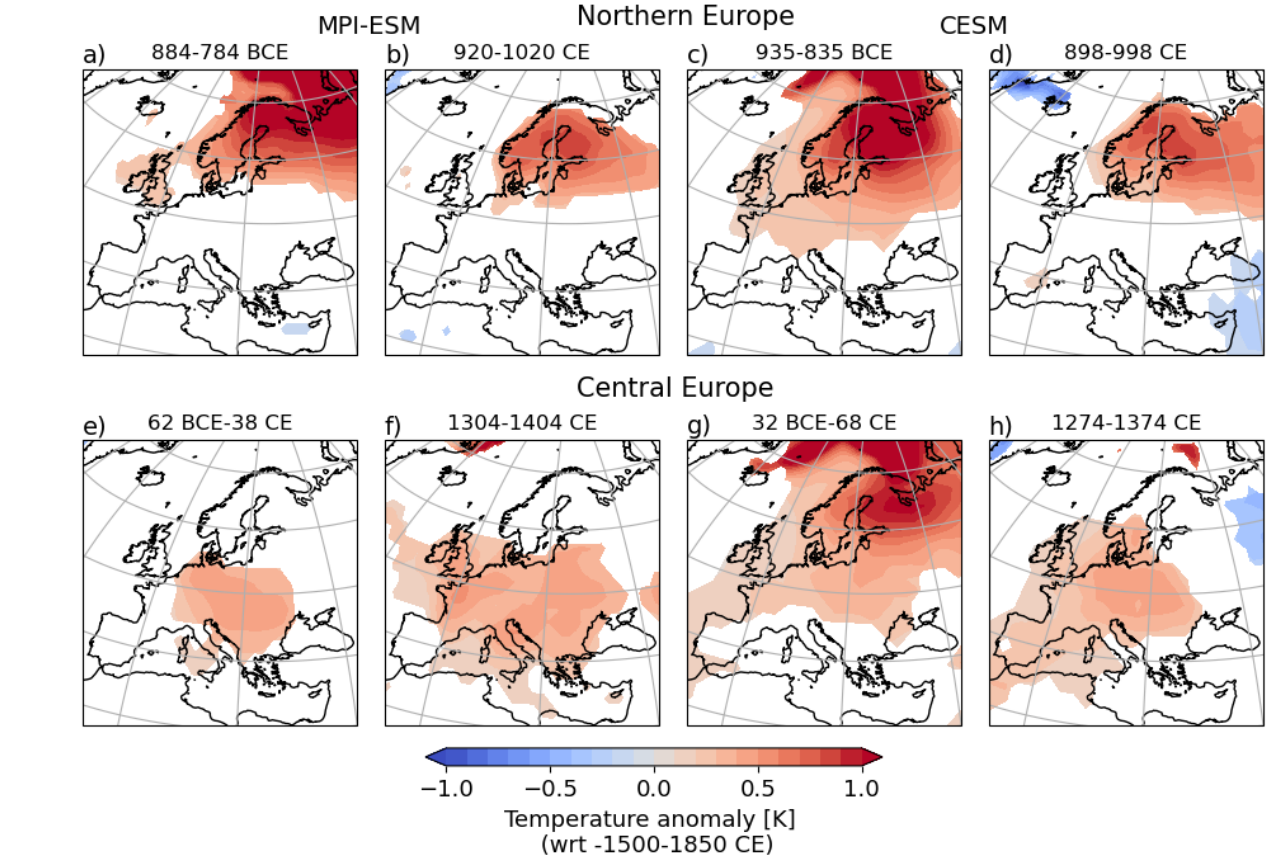

Figure 6. Spatial comparison for selected 100-year warm periods (mean) in MPI (a,b,e,f) and CESM (c,d,g,h) for Northern Europe (a-d) and Central Europe (e-h). Temperature anomalies are with respect to the 1500 BCE - 1850 CE mean from the control simulations.